Supplementary methods 1. Hypothalamic samples metabolomic analysis details.

Hypothalamus samples were processed at Metabolon, Inc using their standard platform protocol described below:

Sample Accessioning: Following receipt, samples were inventoried and immediately stored at -80°C. Each sample received was accessioned into the Metabolon LIMS system and was assigned by the LIMS a unique identifier that was associated with the original source identifier only. This identifier was used to track all sample handling, tasks, results, etc. The samples (and all derived aliquots) were tracked by the LIMS system. All portions of any sample were automatically assigned their own unique identifiers by the LIMS when a new task was created; the relationship of these samples was also tracked. All samples were maintained at -80°C until processed.

Sample Preparation: Samples were prepared using the automated MicroLab STAR® system from Hamilton Company. Several recovery standards were added prior to the first step in the extraction process for QC purposes. To remove protein, dissociate small molecules bound to protein or trapped in the precipitated protein matrix, and to recover chemically diverse metabolites, proteins were precipitated with methanol under vigorous shaking for 2 min (Glen Mills GenoGrinder 2000) followed by centrifugation. The resulting extract was divided into five fractions: two for analysis by two separate reverse phase (RP)/UPLC-MS/MS methods with positive ion mode electrospray ionization (ESI), one for analysis by RP/UPLC-MS/MS with negative ion mode ESI, one for analysis by HILIC/UPLC-MS/MS with negative ion mode ESI, and one sample was reserved for backup. Samples were placed briefly on a TurboVap® (Zymark) to remove the organic solvent. The sample extracts were stored overnight under nitrogen before preparation for analysis.

QA/QC: Several types of controls were analyzed in concert with the experimental samples: a pooled matrix sample generated by taking a small volume of each experimental sample (or alternatively, use of a pool of well-characterized human plasma) served as a technical replicate throughout the data set; extracted water samples served as process blanks; and a cocktail of QC standards that were carefully chosen not to interfere with the measurement of endogenous compounds were spiked into every analyzed sample, allowed instrument performance monitoring and aided chromatographic alignment. Tables 1 and 2 below describe these QC samples and standards. Instrument variability was determined by calculating the median relative standard deviation (RSD) for the standards that were added to each sample prior to injection into the mass spectrometers. Overall process variability was determined by calculating the median RSD for all endogenous metabolites (i.e., non-instrument standards) present in 100% of the pooled matrix samples. Experimental samples were randomized across the platform run with QC samples spaced evenly among the injections, as outlined below in Figure 1.

Table 1: Description of Metabolon QC Samples.

Type	Description	Purpose
MTRX	Large pool of human plasma maintained by Metabolon that has been characterized extensively.	Assure that all aspects of the Metabolon process are operating within specifications.
CMTRX	Pool created by taking a small aliquot from every customer sample.	Assess the effect of a non-plasma matrix on the Metabolon process and distinguish biological variability from process variability.
PRCS	Aliquot of ultra-pure water	Process Blank used to assess the contribution to compound signals from the process.
SOLV	Aliquot of solvents used in extraction.	Solvent Blank used to segregate contamination sources in the extraction.

Table 2: Metabolon QC Standards.

Type	Description	Purpose
RS	Recovery Standard	Assess variability and verify performance of extraction and instrumentation.
IS	Internal Standard	Assess variability and performance of instrument.

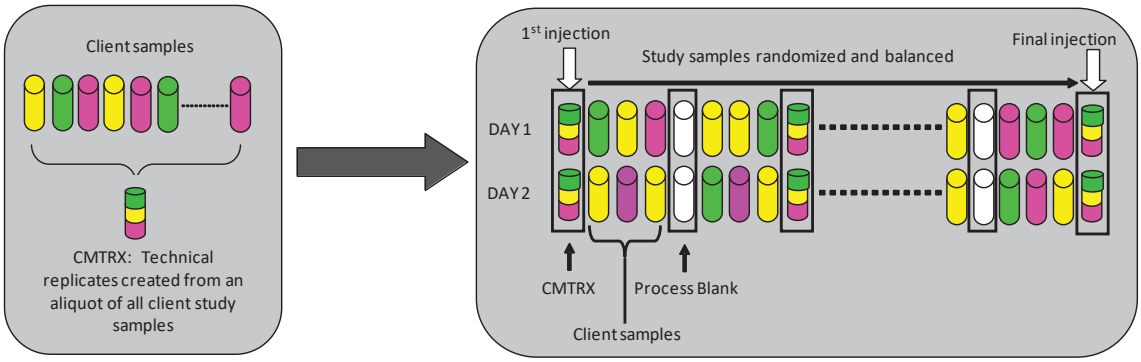

Figure 1. Preparation of client-specific technical replicates. A small aliquot of each client sample (colored cylinders) is pooled to create a CMTRX technical replicate sample (multi-colored cylinder), which is then injected periodically throughout the platform run. Variability among consistently detected biochemicals can be used to calculate an estimate of overall process and platform variability.

Ultrahigh Performance Liquid Chromatography-Tandem Mass Spectroscopy (UPLC-MS/MS): All methods utilized a Waters ACQUITY ultra-performance liquid chromatography (UPLC) and a Thermo Scientific Q-Exactive high resolution/accurate mass spectrometer interfaced with a heated electrospray ionization (HESI-II) source and Orbitrap mass analyzer operated at 35,000 mass resolution. The sample extract was dried then reconstituted in solvents compatible to each of the four methods. Each reconstitution solvent contained a series of standards at fixed concentrations to ensure injection and chromatographic consistency. One aliquot was analyzed using acidic positive ion conditions, chromatographically optimized for

more hydrophilic compounds. In this method, the extract was gradient eluted from a C18 column (Waters UPLC BEH C18-2.1x100 mm, 1.7 µm) using water and methanol, containing 0.05% perfluoropentanoic acid (PFPA) and 0.1% formic acid (FA). Another aliquot was also analyzed using acidic positive ion conditions, however it was chromatographically optimized for more hydrophobic compounds. In this method, the extract was gradient eluted from the same afore mentioned C18 column using methanol, acetonitrile, water, 0.05% PFPA and 0.01% FA and was operated at an overall higher organic content. Another aliquot was analyzed using basic negative ion optimized conditions using a separate dedicated C18 column. The basic extracts were gradient eluted from the column using methanol and water, however with 6.5mM Ammonium Bicarbonate at pH 8. The fourth aliquot was analyzed via negative ionization following elution from a HILIC column (Waters UPLC BEH Amide 2.1x150 mm, 1.7 µm) using a gradient consisting of water and acetonitrile with 10mM Ammonium Formate, pH 10.8. The MS analysis alternated between MS and data-dependent MSn scans using dynamic exclusion. The scan range varied slighted between methods but covered 70-1000 m/z. Raw data files are archived and extracted as described below.

Bioinformatics: The informatics system consisted of four major components, the Laboratory Information Management System (LIMS), the data extraction and peak-identification software, data processing tools for QC and compound identification, and a collection of information interpretation and visualization tools for use by data analysts. The hardware and software foundations for these informatics components were the LAN backbone, and a database server running Oracle 10.2.0.1 Enterprise Edition.

LIMS: The purpose of the Metabolon LIMS system was to enable fully auditable laboratory automation through a secure, easy to use, and highly specialized system. The scope of the Metabolon LIMS system encompasses sample accessioning, sample preparation and instrumental analysis and reporting and advanced data analysis. All of the subsequent software systems are grounded in the LIMS data structures. It has been modified to leverage and interface with the in-house information extraction and data visualization systems, as well as third party instrumentation and data analysis software.

Data Extraction and Compound Identification: Raw data was extracted, peak-identified and QC processed using Metabolon's hardware and software. These systems are built on a web-service platform utilizing Microsoft's .NET technologies, which run on high-performance application servers and fiber-channel storage arrays in clusters to provide active failover and load-balancing. Compounds were identified by comparison to library entries of purified standards or recurrent unknown entities. Metabolon maintains a library based on authenticated standards that contains the retention time/index (RI), mass to charge ratio (m/z), and chromatographic data (including MS/MS spectral data) on all molecules present in the library. Furthermore, biochemical identifications are based on three criteria: retention index within a narrow RI window of the proposed identification, accurate mass match to the library +/- 10 ppm, and the MS/MS forward and reverse scores between the experimental data and authentic standards. The MS/MS scores are based on a comparison of the ions present in the experimental spectrum to the ions present in the library spectrum. While there may be similarities between these molecules based on one of these factors, the use of all three data points can be utilized to distinguish and differentiate biochemicals. More than 3300 commercially available purified standard compounds have been acquired and registered into LIMS for analysis on all platforms for determination of their analytical characteristics. Additional mass spectral entries have been created for structurally unnamed biochemicals, which have been identified by virtue of their recurrent nature (both chromatographic and mass spectral). These compounds have the potential to be identified by future acquisition of a matching purified standard or by classical structural analysis.

Curation: A variety of curation procedures were carried out to ensure that a high quality data set was made available for statistical analysis and data interpretation. The QC and curation processes were designed to ensure accurate and consistent identification of true chemical entities, and to remove those representing system artifacts, mis-assignments, and background noise. Metabolon data analysts use proprietary visualization and interpretation software to confirm the consistency of peak identification among the various samples. Library matches for each compound were checked for each sample and corrected if necessary.

Metabolite Quantification and Data Normalization: Peaks were quantified using area-under-the-curve. For studies spanning multiple days, a data normalization step was performed to correct variation resulting from instrument inter-day tuning differences. Essentially, each compound was corrected in run-day blocks by registering the medians to equal one (1.00) and normalizing each data point proportionately (termed the "block correction"; Figure 2 below). For studies that did not require more than one day of analysis, no normalization is necessary, other than for purposes of data visualization. In certain instances, biochemical data may have been normalized to an additional factor (e.g., cell counts, total protein as determined by Bradford assay, osmolality, etc.) to account for differences in metabolite levels due to differences in the amount of material present in each sample.

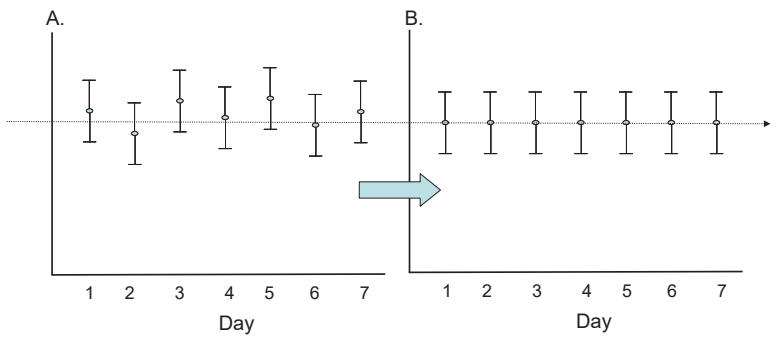

Figure 2: Visualization of data normalization steps for a multiday platform run.

Supplementary methods 2. Caecal content untargeted metabolomic analysis details.

Caecal water samples preparation:

Caecal contents were grinded (Precellys24; 5000rpm for 2x30sec, 20sec break) in 2mL impact resistant tubes filled with 0.6mL of beads (ZR Bashing Bead Lysis Tubes (0.1 and 0.5mm)) and MilliQ water (1mL per 100mg of sample). Grinded samples were then ultracentrifuged (171500g for 2 hours at 4°C). 2µL of NaN3 solution (100mg.mL^{-1}) was added per mL of supernatant. These caecal water samples were stocked at -80°C before untargeted metabolomics analysis.

GC sample preparation:

Caecal water samples were frozen and stored at -80°C for further analysis. Caecal water samples were thawed from -80°C to 4°C overnight. 600 µL of ice-cold methanol (-20°C) were added to 300µL caecal water sample for each sample in Eppendorf tube. The mixture was vortexed. After precipitation of the proteins, samples were kept in the freezer at -20°C for half an hour and then centrifuged (Sigma 3-16PK, Fischer Bioblok Scientific) at 15 000 rpm for 10 min at 4°C. 800µL of supernatant were transferred in a brown glass vial of 2mL before addition

of 10 µL of [13C1]-L-valine (200 µg.mL^{-1}) and evaporation under EZ2.3 Genevac (Biopharma Technologies France). At the same time, a control derivatization sample (for which caecal water was substituted by milliQ water) was prepared in order to remove the background noise produced during sample preprocessing, derivatization, and Gas Chromatography/Mass Spectrometry (GC/MS) analysis. The obtained dry residues were dissolved by adding 80 µL of methoxylamine hydrochloride solution (15 mg.mL^{-1} in pyridine) to each vial, vortexed vigorously for 1 min and incubated for 24h at 37 °C in order to inhibit the cyclization of reducing sugars and the decarboxylation of α-keto acids. Then, 80µL of N,O-bis(trimethylsilyl)trifluoroacetamide (BSTFA) with 1% trimethylchlorosilane (TMCS) as catalyst were added in the mixture and derivatized for 60 min at 70°C. Before injection, 50µL of derivatized mixture (by trimethylsilylation) were transferred in a glass vial containing 100µL of heptane. In a similar manner, a sample pool was formed from 10µL of each extracted and derivatized sample to monitor the drift of the spectrometer during GC-MS analysis.

Analytical sequences:

Injection order was randomized using a William's latin squares strategy. Four heptane blanks were injected at the beginning of each sequence, followed by four pool samples, and then one pool sample and one derivatization control sample after each set of 10 samples. Initial tuning and calibrating of the system were performed using perfluorotributylamine (PFTBA). Also, a calibration was made between each sample.

Gas chromatography and mass spectrometry:

Untargeted metabolic analysis were performed on an Agilent 7890B Gas Chromatograph, equipped with a 7693A Injector (SSL) Auto-Sampler (Agilent Technologies, Inc), coupled to an Agilent QTOF 7200 (Quadripole Time Of Flight) mass spectrometer. Separation was achieved on a fused silica column HP-5MS UI 30m x 0.25mm i.d. chemically bonded with a 5% phenyl-95% methylpolysiloxane cross-linked stationary phase (0.25 µm film thickness) (Agilent J & W Scientific, Folsom, CA, USA). Helium was used as a carrier gas at a flow rate of 1 ml.min^{-1}. 2 µl of derivatized sample were injected using 1:20 split. Temperatures of injector, transfer line, and electron impact (EI) ion source were set to 250 °C, 280 °C and 230 °C, respectively. The initial oven temperature was 60 °C for 2 min, ramped to 140°C at a rate of 10°C per minute, to 240°C at a rate of 4°C per minute, to 300°C at a rate of 10 °C per minute and finally held at 300°C for 8 min. The total run time was 49 min. Agilent ''retention time locking" (RTL) was applied to control the reproducibility of retention times (RT). [13C1]-L-valine (ISTD) was used to lock GC method (Gao *et al.*, 2010). The electron energy was 70 eV and mass data were collected in a full scan mode (m/z 55-700) using a resolution of 7000 (full width at half maximum) to 464 m/z. Acquisition rate was 5 spectra per second with acquisition time of 200ms per spectrum. Raw data files were transformed to mzdata files using Masshunter software (Agilent).

Data processing:

The obtained mzdata files were imported under the Galaxy web-based platform Workflow4Metabolomics (W4M) (Giacomoni et al., 2015).

Mzdata files were processed using XCMS (Smith et al., 2006), which includes several steps that led to a data matrix containing retention times, m/z ratio and peak intensities (Migné et al., 2018). These steps consisted of noise filtering, automatic peak detection and chromatographic alignment allowing the appropriate comparison of multiple samples by further processing methods and quality controls with signal drift and batch effect correction.

To note, mass fragments with m/z-values of 73.0418, 74.0421, 75.0317, 76.0220 and 147.0716 are not specific for the differentiation of compounds. These mass fragments predominantly result from the derivatization reagent (TMS) and were thus excluded from workflow analysis.

Analytical correlations were filtered using the 'Metabolites Correlation Analysis' tool (Galaxy Version 1.0.1) with a correlation coefficient threshold of 0.9.

After these processing steps, 785 ions from caecal waters metabolome remained in datasets for statistical analyses.

Metabolite identification:

At first an in-house database was used to identify metabolites: pure compounds (standards) were previously analyzed in the same analytical conditions on the same instrument. The remaining unknown compounds were identified based on their exact masses that were compared to those registered in MassBank (https://www.massbank.eu) and HuMan DataBase (HMDB) (www.hmdb.ca) (with nominal masses and masses error 0.3 Da) or National Institute of Standards and Technology (NIST) library. Deconvolution of the raw data files was achieved using Agilent MassHunter software package (qualitative Analysis B.07.01) and the mass spectral data was compared against a personal compound database library (Agilent MassHunter Personal Compound Database and Library (PCDL) version B.07.00) containing spectra of pure compounds (standards) previously analyzed on the same instrument and NIST library.

As in Metabolon method (supplementary methods 1), obtained data were normalized by setting the median of each ion to 1. T0 values were considered as the control values and set to 1 to calculate the fold-changes between time-groups of each ion.

Supplementary method 3.

16S rRNA gene sequencing analysis

Reads obtained after 16S rRNA gene sequencing from caecal content were filtered and taxonomic affiliation (SILVA database version 132) was performed using dada2 R package v.1.14.0 on R v.3.6.1 (ref. 1). Data were normalized using Geometric Mean of Pairwise Ratios method with the GMPR R package v.0.1.3 (ref. 1). Diversity measures (Shannon index from raw data and Bray-Curtis distance from normalized data) as well as composition analysis were performed using the phyloseq R package v.1.30.0 (ref. 3).

Data integration using the mixOmics R package

PLS-DA were performed on normalized metabolomic data using the mixOmics R package v.6.10.1 (M-fold cross-validation (5 folds, 100 repeats)) and the number of components corresponding to the lowest classification error rate obtained according to the balanced error rate was selected for each data set (4). Model performance was assessed using the perf function of mixOmics R package. PERMANOVA tests were performed between pairs of groups on PLS-DA coordinates with the vegan R package v.2.5-6. Hypothalamic metabolites of interest for further data integration were selected based on PLS-DA Variable Importance in Projection (VIP) scores (superior to 1 for components 1 and 2).

Data integration using the MiBiOmics web application.

To perform data integration, the web application MiBiOmics (5), based on Weighted Correlation Network Analysis method (WGCNA) (42) was used. Briefly, for each dataset, sub-networks of highly correlated Operational Taxonomic Units (OTUs) or metabolites were built. Each sub-network from one dataset was then correlated to sub-networks from the two other datasets. Hypothalamic sub-networks containing inflammation related metabolites were selected and OTU and caecal metabolites sub-networks that were highly correlated with them were kept. Specific hypothalamic metabolites, caecal metabolites and OTUs from these selected sub-networks that were highly correlated with each other were kept to build the final network. One network per dataset (microbiota, caecal metabolome and hypothalamic metabolome) was built by correlating all variables together using correlation parameters listed in table below.

Dataset	Softpower	Minimal module size	Type of correlation
Caecal microbiota	7	6	Biweight midcorrelation
Caecal ions	12	6	Spearman
Hypothalamic metabolites	14	6	Biweight midcorrelation

Parameters used to build the WGCNA network from each dataset. All networks were signed.

Inside each network, sub-networks (called “modules”) of highly correlated variables (OTUs, ions or metabolites) were used to find inter-sub-networks correlations between datasets. Hypothalamic sub-networks containing previously identified hypothalamic metabolites, using VIP score after PLS-DA, were retained. Sub-networks from the two other datasets that had a Pearson correlation coefficient between them and with the selected hypothalamic sub-networks superior to 0.6 (absolute value) were kept. Then, correlations between variables of these selected sub-networks (OTUs, ions or metabolites) that were also superior to 0.6 (absolute value) were selected to build the final network. The taxonomic affiliations of OTUs retained after this selection were more precisely identified using the BLASTn tool on 16S rRNA gene reference database on the NCBI website (first hits presenting the higher percentage of identity and query cover, as well as the lowest E-value, were retained).

Supplementary Materials

Supplementary table 1. Composition of the experimental diets. WD: Western diet.

	Experiment 1		**Experiment 2**		**Experiment 3**	
	Chow	**WD**	**Chow**	**WD**	**Chow**	**WD**
Food reference #	Labdiet 5008	D12451	SDS N°3	D12451	SAFE A03	SAFE 245HF
Energy density *(kcal.g^{-1})*	3.4	4.7	3.6	4.7	3.3	4.7
Carbohydrate *(% energy)*	58	35	61.5	35	61.3	36.8
Protein *(% energy)*	29	20	27	20	25.2	17.3
Fat *(% energy)*	13	45	11.5	45	13.5	45.9
Irradiation	-	-	-	-	45kGy	45kGy

Supplementary Materials

Supplementary table 2. References of primers or assay-on-demand (AOD) of genes which levels were determined by qPCR in the hypothalamus of experiment 3 rats. Gene names, primers sequences (forward and reverse) and hybridization temperatures (Tm, in °C) of each primer are listed for genes involved in oxidative stress (SYBR green technology). AOD are referenced for genes involved in inflammation (TaqMan technology). F: forward. R: reverse.

Type	Gene	Protein	Technology	Forward (F; 5'-3')	Reverse (R; 5'-3')	Tm (F-R; °C)	AOD
Reference genes	***actb***	β-actin	SYBR green	ctaaggccaaccgtgaaaag	accagaggcatacagggaca	57-60	-
	rplp0	Ribosomal protein lateral stalk subunit P0	SYBR green	cgagaagacctctttcttccaa	agtctttatcagctgcacatcg	58-59	-
	rps18	18S	SYBR green	cttccacaggaggcctacac	tgaaacttctcggggatca	59-59	-
	actb	β-actin	TaqMan	-	-	-	Rn00667869_m1
Oxidative stress	***gcs***	Gamma-glutamylcysteine synthetase	SYBR green	gactgttgccaggtggatga	ttgtgggcaactggaacact	60-60	-
	gs	Glutathione synthetase	SYBR green	agcgtgccatagagaacgag	ggcatgtagccatctcggaa	60-60	-
	gst	Glutathione S-transferase	SYBR green	tctgaaaactcgggatgacc	caccagcttcatcccatca	57-57	-
	sod2	Superoxide dismutase 2	SYBR green	ggccatatcaatcacagcatt	tagcctccagcaactctcct	57-60	-
	sod3	Superoxide dismutase 3	SYBR green	cttgggagagcttgtcaggt	caccagtagcaggttgcaga	59-60	-
	glrx	Glutaredoxin-1	SYBR green	caacagaatggggagctgac	ggacgactgctgtcagtatgg	59-60	-
	gpx1	Glutathione peroxidase 1	SYBR green	tttcccgtgcaatcagttc	ggacatacttgagggaattcaga	56-58	-
Inflammation	***iba1***	Ionized calcium binding adapter molecule 1	SYBR green	cagacgcaccctctgatgt	ctccaagaatggggtgagc	59-58	-
	ccl2	Chemokine ligand 2	TaqMan	-	-	-	Rn00580555_m1
	tnfα	Tumor necrosis factor α	TaqMan	-	-	-	Rn01525859_g1
	il1β	Interleukin-1β	TaqMan	-	-	-	Rn00580432_m1
	il6	Interleukin-6	TaqMan	-	-	-	Rn01410330_m1

Supplementary table 3. Hypothalamic metabolites retained after PLS-DA. Metabolites were ordered according to their VIP scores for components 1 (comp1) and 2 (comp2) combined, with a filter on VIP score > 1. Data were then sorted in decreasing order according to comp1. Blue: arginine metabolism; yellow brown: lipids; red: redox homeostasis; green: cell membrane remodelling.

	VIP score				
Metabolite	comp1	comp2	comp3	comp4	comp5
trigonelline (N'-methylnicotinate)	2.967099	2.327452	1.96734	1.891237	1.824557
N-delta-acetylornithine	2.677039	2.231608	1.890086	1.93996	1.871615
4-guanidinobutanoate	2.612261	1.899909	1.622304	1.95395	1.893464
stachydrine	2.573225	1.893569	1.645883	1.438057	1.392574
dimethylarginine (SDMA + ADMA)	2.391624	1.811732	1.524908	1.548708	1.51177
adenosine 2'-monophosphate (2'-AMP)	2.375548	1.723198	1.526331	1.440993	1.39535
1-methylhistamine	2.345086	1.701932	1.430518	1.290088	1.247398
chiro-inositol	2.279936	1.757628	1.657332	1.81998	1.757433
N-acetylmethionine	2.23257	1.628505	1.410716	1.267446	1.228946
adenosine	2.225997	1.630498	1.484653	1.282629	1.237641
phenol sulfate	2.184963	1.798397	1.602626	1.388193	1.340937
1,2-dilinoleoyl-GPC (18:2/18:2)	2.161965	1.697343	1.43605	1.241138	1.197351
myo-inositol	2.107868	1.660423	1.41547	1.330963	1.284134
dihydroxyacetone phosphate (DHAP)	2.078272	1.61347	1.402904	1.221359	1.198442
gamma-glutamylphenylalanine	2.077705	1.754754	1.577668	1.362123	1.321503
ascorbate (Vitamin C)	2.07337	1.671731	1.422469	1.306378	1.278259
sedoheptulose-7-phosphate	2.043451	1.545887	1.336088	1.16735	1.13327
sphingomyelin (d18:1/24:1, d18:2/24:0)*	2.000773	1.537874	1.298484	1.16264	1.128468
N-acetylarginine	1.998233	1.680013	1.71195	1.481449	1.46866
ornithine	1.988632	1.827345	1.540504	1.34175	1.328292
sphingosine	1.986259	1.665612	1.506332	1.305795	1.278874
betaine	1.973483	1.517926	1.693891	1.473127	1.421958
gamma-glutamylglycine	1.957683	1.533044	1.296337	1.12463	1.135467
glutamate	1.95433	1.42138	1.196076	1.035399	1.026058
isoleucylglycine	1.941739	1.686504	1.442637	1.264458	1.219857
ophthalmate	1.941198	1.946435	1.820218	1.589336	1.53427
gamma-tocopherol/beta-tocopherol	1.891518	1.865859	1.569866	1.453405	1.428843
mannose	1.885384	1.409579	1.306274	1.138261	1.098879
pyridoxal	1.843703	1.726446	1.464267	1.272146	1.229361
N-acetylmethionine sulfoxide	1.821895	1.326288	1.253452	1.23801	1.194445
S-1-pyrroline-5-carboxylate	1.810042	1.569968	1.328378	1.243542	1.264332
argininate*	1.809936	1.777539	1.540621	1.800483	1.743385
S-adenosylhomocysteine (SAH)	1.786148	1.384803	1.220156	1.131286	1.098178
glycylleucine	1.771185	1.303137	1.097785	1.10654	1.102127
saccharopine	1.76639	1.684837	1.525747	1.406948	1.399582
N-stearoyl-sphingosine (d18:1/18:0)*	1.753165	1.449217	1.259461	1.099504	1.060755

riboflavin (Vitamin B2)	1.749434	1.274456	1.075587	1.096261	1.073063
3-indoxyl sulfate	1.743829	2.032844	1.71902	1.484597	1.43252
sphingomyelin (d18:2/23:0, d18:1/23:1, d17:1/24:1)*	1.741648	1.432937	1.315633	1.137042	1.113173
cysteine-glutathione disulfide	1.724007	1.528291	1.358179	1.172948	1.135616
phosphate	1.719617	1.281429	1.085497	1.08429	1.073132
1-methylimidazoleacetate	1.677472	1.242228	1.264018	1.092408	1.084649
N-palmitoyl-sphinganine (d18:0/16:0)	1.672615	1.306477	1.113162	1.15022	1.114158
nicotinamide	1.670557	1.471288	1.24773	1.132755	1.151215
adenine	1.66239	1.238584	1.171366	1.07014	1.076761
glycosyl ceramide (d18:2/24:1, d18:1/24:2)*	1.636255	1.248299	1.245039	1.100209	1.144937
glycosyl-N-erucoyl-sphingosine (d18:1/22:1)*	1.627778	1.231273	1.185623	1.043981	1.161701
1-(1-enyl-oleoyl)-2-oleoyl-GPE (P-18:1/18:1)*	1.622995	1.213792	1.12713	0.989152	1.029495
homoarginine	1.622429	1.38654	1.342804	1.628548	1.578586
ribose	1.621264	1.448516	1.222522	1.397801	1.359072
tyrosylglycine	1.614729	1.415211	1.198724	1.042181	1.071046
palmitoylcarnitine (C16)	1.6142	1.389293	1.35277	1.174926	1.145858
N-acetylleucine	1.608175	1.695569	1.523677	1.322244	1.291133
hypotaurine	1.6039	1.227555	1.207236	1.057527	1.021936
eicosanoylsphingosine (d20:1)*	1.601746	1.595686	1.402888	1.212961	1.184796
1-stearoyl-2-oleoyl-GPS (18:0/18:1)	1.588568	1.26979	1.345748	1.168816	1.145567
allantoin	1.583892	1.393437	1.423015	1.307729	1.272188
5-oxoproline	1.582148	1.688905	1.438293	1.382746	1.341958
betaine aldehyde	1.575888	1.143192	1.003153	1.129353	1.154183
spermidine	1.547189	1.150498	0.992662	0.891167	1.011594
allo-threonine	1.516206	1.146866	1.025229	0.888768	1.041244
arabitol/xylitol	1.507938	1.281318	1.166077	1.109923	1.177597
uracil	1.506264	1.654881	1.391302	1.203423	1.182282
2'-deoxyuridine	1.501329	1.177006	1.061819	1.05423	1.063853
oxalate (ethanedioate)	1.479072	1.076535	1.124774	1.255107	1.289749
1-oleoyl-2-arachidonoyl-GPE (18:1/20:4)*	1.477477	1.158108	1.436536	1.346282	1.298883
5-methyl-2'-deoxycytidine	1.471903	1.289128	1.959871	1.709547	1.649568
S-lactoylglutathione	1.46841	1.064838	1.186611	1.028412	1.026455
gamma-glutamyltryptophan	1.453006	1.143712	1.007564	0.956407	1.01829
gamma-glutamylleucine	1.449489	1.081773	1.428944	1.26728	1.275393
spermine	1.426909	1.068694	0.923797	0.874101	1.00591
1-(1-enyl-stearoyl)-2-arachidonoyl-GPE (P-18:0/20:4)*	1.426696	1.092009	1.234357	1.081395	1.053873
stearoyl-arachidonoyl-glycerol (18:0/20:4) [2]*	1.420048	1.511213	1.272818	1.216116	1.192991
carboxyethyl-GABA	1.415438	1.045962	0.911216	1.235809	1.210729
glucuronate	1.409812	1.102581	1.336281	1.517941	1.464638
lignoceroyl sphingomyelin (d18:1/24:0)	1.401477	1.017929	1.075266	1.080045	1.060716
1-methylguanidine	1.397159	1.444218	1.267171	1.095638	1.110505
4-cholesten-3-one	1.393239	1.594932	1.481809	1.296989	1.300039

glutathione, oxidized (GSSG)	1.373266	1.463682	1.230087	1.160986	1.138975
myristoylcarnitine (C14)	1.372085	1.082066	1.21196	1.051136	1.020533
1-(1-enyl-oleoyl)-GPE (P-18:1)*	1.371503	1.150986	1.142514	1.016956	1.003323
arachidonoylcarnitine (C20:4)	1.340738	1.233749	1.048129	1.078739	1.085302
oleoylcarnitine (C18:1)	1.337515	1.209781	1.203307	1.050469	1.01479
uridine	1.293719	1.094673	0.94187	0.813087	1.074955
orotidine	1.272032	2.04917	1.724908	1.492798	1.483633
13-HODE + 9-HODE	1.269184	1.661406	1.446336	1.287425	1.242673
gamma-glutamylhistidine	1.234133	1.23691	1.250944	1.111834	1.11339
hypoxanthine	1.185649	1.382172	1.176199	1.045001	1.020348
urea	1.18335	1.539447	1.519725	1.751115	1.710412
1-methylnicotinamide	1.180345	1.041064	0.910026	1.034238	1.024507
glycosyl-N-palmitoyl-sphingosine (d18:1/16:0)	1.178191	1.431418	1.335671	1.15814	1.117836
2-arachidonoylglycerol (20:4)	1.163004	1.592533	1.358337	1.23168	1.201949
gamma-glutamylvaline	1.157768	1.002545	1.009476	0.986275	1.005765
glycerophosphorylcholine (GPC)	1.139032	1.452545	1.314663	1.136428	1.108398
2-hydroxybutyrate/2-hydroxyisobutyrate	1.103702	1.998238	1.680059	1.454898	1.403773
1-dihomo-linolenylglycerol (20:3)	1.088362	1.267461	1.127794	1.229765	1.18767
citrulline	1.083079	1.545888	1.308442	1.142637	1.222846
myristate (14:0)	1.063034	1.377166	1.276282	1.116959	1.07803
1-(1-enyl-stearoyl)-GPE (P-18:0)*	1.042186	1.207819	1.465591	1.43497	1.386639
gamma-glutamylglutamine	1.017483	1.11443	0.949528	1.071438	1.073302
1-arachidonylglycerol (20:4)	1.001585	1.044528	1.168077	1.486293	1.44045

Supplementary Materials

Supplementary table 4. ANOVA and post-hoc tests results on the significantly impacted metabolites after pathway enrichment. Metabolites were selected by the Metabolon platform after performing metabolic pathway enrichment. Values correspond to fold-change between the considered time group and T0, after setting the median to 1 for each metabolite. T0 values are set to 1. Significant result after ANOVA are indicated in the ANOVA column by a dark blue fill while tendencies are indicated by a light blue fill. A dark green or red background means that the post-hoc test result between the considered time and T0 is significant, respectively with a decrease or an increase in the considered metabolite level compared to T0. A light green or light red background means that the post-hoc test resulted in a tendency between the considered time and T0, respectively with a tendency to a decrease or an increase for this metabolite level compared to T0. Two different letters indicate a significant difference. An asterisk (*) indicates compounds that have not been officially confirmed based on a standard, but with confidence in its identity according to the metabolomic platform.

Pathway	Metabolite	ANOVA	T0	T2H	TD1	TD2	TD4
Redox homeostasis	ophthalmate	Significant	1	1.25	1.61	3.72	3.23
			a	a	a	bc	c
	gamma-glutamylphenylalanine	Significant	1	0.99	0.74	0.6	0.59
			a	ab	bcd	cd	d
	gamma-glutamyltryptophan	Significant	1	0.99	0.58	0.53	0.57
			a	a	b	b	b
	5-oxoproline	Significant	1	0.92	0.82	0.8	0.82
			a	ab	c	bc	bc
	2-hydroxybutyrate/2-hydroxyisobutyrate	Significant	1	1.22	1.2	1.34	1.32
			a	b	b	b	b
	gamma-glutamylglycine	Significant	1	1	0.82	0.84	0.79
			a	a	b	b	b
	13-hydroxy-9,11-octadecadienoic acid + 9-Hydroxy-10,12-octadecadienoic acid	Significant	1	1.36	1.63	1.83	1.63
			a	ab	b	b	b
	gamma-glutamylleucine	Significant	1	1.07	0.97	0.81	0.87
			a	a	abc	bc	c
	gamma-glutamylglutamine	Significant	1	1.12	0.92	0.99	1
			ab	a	b	b	ab
	glutamate	Tendency	1	0.94	0.99	1.03	1
			ab	a	ab	b	b
	glycine	Tendency	1	0.98	0.94	0.95	0.93
			a	ab	b	ab	b
	glutathione, oxidized (GSSG)	Tendency	1	1.07	1.15	1.27	1.16
			a	a	ab	b	ab
	gamma-glutamylvaline	Tendency	1	1.07	0.92	1.04	0.91
			ab	a	b	ab	b
	gamma-glutamylglutamate	Tendency	1	1.01	0.9	0.89	0.89
			ab	a	ab	b	b
Cell membrane metabolism	diacylglycerol (16:1/18:2 [2], 16:0/18:3 [1])*	Tendency	1	6.51	1.91	1.34	2.61
			ab	cd	abcd	bcd	d
	choline phosphate	Significant	1	1.02	0.94	0.97	0.93
			ab	b	ac	abc	c
	1,2-dilinoleoyl-GPC (18:2/18:2)	Significant	1	1.04	0.8	0.77	0.72
			a	a	b	b	b
	1-linoleoyl-2-arachidonoyl-GPC (18:2/20:4n6)*	Significant	1	0.96	0.85	0.92	0.86
			a	ab	c	abc	bc
	glycerophosphorylcholine (GPC)	Significant	1	1.12	1.12	1.39	1.26
			a	abc	abd	c	cd
	1-palmitoyl-2-linoleoyl-GPC (16:0/18:2)	Tendency	1	0.96	0.92	0.97	0.94
			a	ab	b	a	ab
	cytidine 5'-monophosphate (5'-CMP)	Tendency	1	1.11	1.04	1.03	0.96

			a	**b**	**ab**	**ab**	**a**
	cytidine-5'-diphosphoethanolamine	**Tendency**	1	0.93	1	**1.18**	1.14
			ab	**b**	**ab**	**a**	**a**
	cytidine 5'-diphosphocholine	**Significant**	1	0.99	0.92	**1.15**	0.98
			a	**a**	**a**	**b**	**a**
	glycerophosphoethanolamine	**Tendency**	1	1.1	1.01	**1.17**	1.09
			ab	**abc**	**b**	**c**	**abc**
Arginin metabolism	urea	**Significant**	1	**0.9**	0.94	**0.83**	**0.73**
			a	ab	a	b	c
	ornithine	**Significant**	1	0.93	**0.79**	**0.77**	**0.75**
			a	a	b	b	b
	homoarginine	**Significant**	1	1	0.92	**1.4**	**1.96**
			a	ab	b	cd	d
	homocitrulline	**Significant**	1	1.17	0.92	1.23	**0.6**
			a	a	a	a	b
	citrulline	**Significant**	1	**0.87**	**0.82**	**0.83**	**0.77**
			a	ab	b	b	b
	spermidine	**Tendency**	1	1.07	0.78	0.84	**0.71**
			a	a	ab	ab	b

Supplementary table 5. Relative abundances values (%) of caecal microbiota families across time. Values are expressed as means ± standard deviation.

Family	T0	T2H	TD1	TD2	TD4
Bacteroidaceae	3.97 ± 2.91	2.38 ± 0.99	4.23 ± 2.34	6.83 ± 3.01	5.47 ± 3.6
Desulfovibrionaceae	3.5 ± 2.45	3.65 ± 2.01	7.37 ± 3.63	9.53 ± 4.03	6.93 ± 4.51
Lachnospiraceae	30.3 ± 6.88	30.6 ± 5.12	18.37 ± 3.42	25.39 ± 11.66	29.54 ± 13.17
Lactobacillaceae	13.03 ± 5.54	9.4 ± 2.83	2.98 ± 2.05	1.31 ± 1.8	0.39 ± 0.3
Muribaculaceae	6.7 ± 1.18	5.3 ± 1.05	3.43 ± 1.59	3.31 ± 1.5	2.43 ± 1.33
Peptostreptococcaceae	9.92 ± 6.57	11.02 ± 5.96	11.2 ± 4.59	11.39 ± 8.78	14.01 ± 15.48
Prevotellaceae	2.68 ± 2.14	4.13 ± 1.81	2.75 ± 2.1	0.8 ± 0.65	0.99 ± 0.86
Rikenellaceae	5.4 ± 3.62	5.32 ± 3.22	5.42 ± 3.49	6.76 ± 4.42	5.71 ± 4.4
Ruminococcaceae	17.58 ± 2.77	21.02 ± 5.33	15.92 ± 5.95	14.67 ± 3.66	13.21 ± 5.3
Tannerellaceae	3.72 ± 2.37	3.22 ± 1.24	7.28 ± 3.82	13.39 ± 6.39	13.23 ± 8.92

Supplementary Materials

Supplementary table 6. Identity of bacteria identified after data integration. The taxonomy of each OTU that was strongly (Pearson correlation coefficient > 0.6 in terms of absolute value) correlated to selected caecal metabolites and hypothalamic oxidative stress-related metabolites was identified using basic local alignment search tool (BLAST) from the National Center for Biotechnology Information (NCBI). First BLAST hits results and characteristics on OTUs identified as positively and strongly correlated with pro-oxidant hypothalamic metabolites after data integration using WGCNA method are listed.

OTU	Description	Max Score	Total Score	Query Cover	E-value	% identity	Accession
17	Uncultured bacterium clone OTU445_L_2_F0_126636 16S ribosomal RNA gene, partial sequence	702	702	100%	0	99.48%	MG858281.1
109	Uncultured bacterium clone JD68 16S ribosomal RNA gene, partial sequence	713	713	100%	0	100.00%	JF794965.1
133	Lactobacillus johnsonii strain 0.1XD8_76 16S ribosomal RNA gene, partial sequence	708	708	100%	0	99.74%	MN081622.1
	Lactobacillus taiwanensis strain 0.1XD42_62 16S ribosomal RNA gene, partial sequence	708	708	100%	0	99.74%	MN081621.1
306	Lactobacillus johnsonii strain 0.1XD8_76 16S ribosomal RNA gene, partial sequence	708	708	100%	0	99.74%	MN081622.1
	Lactobacillus taiwanensis strain 0.1XD42_62 16S ribosomal RNA gene, partial sequence	708	708	100%	0	99.74%	MN081621.1
359	Lactobacillus johnsonii strain 0.1XD8_76 16S ribosomal RNA gene, partial sequence	708	708	100%	0	99.74%	MN081622.1
	Lactobacillus taiwanensis strain 0.1XD42_62 16S ribosomal RNA gene, partial sequence	708	708	100%	0	99.74%	MN081621.1
20	Uncultured bacterium clone denovo46872_N21_133494 16S ribosomal RNA gene, partial sequence	713	713	100%	0	100.00%	MF257433.1
250	Eubacterium ventriosum strain ATCC 27560 16S ribosomal RNA, partial sequence	660	660	100%	0	97.15%	NR_118670.1
404	Lactobacillus taiwanensis strain BCRC 17755 16S ribosomal RNA, partial sequence	708	708	100%	0	99.74%	NR_044507.1
36	Ruminococcus albus 7 = DSM 20455 16S ribosomal RNA, partial sequence	569	569	100%	3.00E-162	93.26%	NR_074399.1
475	Escherichia fergusonii ATCC 35469 16S ribosomal RNA, complete sequence	713	713	100%	0	100.00%	NR_074902.1
121	[Clostridium] saccharogumia strain SDG-Mt85-3Db 16S ribosomal RNA, partial sequence	691	691	100%	0	98.96%	NR_043550.1
441	Lactobacillus taiwanensis strain BCRC 17755 16S ribosomal RNA, partial sequence	708	708	100%	0	99.74%	NR_044507.1
230	Vallitalea pronyensis strain FatNI3 16S ribosomal RNA, partial sequence	438	438	99%	9.00E-123	87.31%	NR_125677.1
79	Muribaculum intestinale strain YL27 16S ribosomal RNA, partial sequence	448	448	99%	1.00E-125	87.89%	NR_144616.1
251	Aminipila butyrica strain FH042 16S ribosomal RNA, partial sequence	630	630	100%	1.00E-180	96.11%	NR_159296.1
300	Murimonas intestini strain SRB-530-5-H 16S ribosomal RNA, partial sequence	664	664	100%	0	97.67%	NR_134772.1
341	Lactobacillus reuteri DSM 20016 16S ribosomal RNA, partial sequence	708	708	100%	0	99.74%	NR_075036.1
379	Lactobacillus taiwanensis strain BCRC 17755 16S ribosomal RNA, partial sequence	708	708	100%	0	99.74%	NR_044507.1
127	Kineothrix alysoides strain KNHs209 16S ribosomal RNA, partial sequence	630	630	100%	1.00E-180	96.11%	NR_156080.1
142	Blautia schinkii strain B 16S ribosomal RNA, partial sequence	643	643	100%	0	96.63%	NR_026312.1
12	Lactobacillus reuteri DSM 20016 16S ribosomal RNA, partial sequence	713	713	100%	0	100.00%	NR_075036.1
161	Anaerotaenia torta strain FH052 16S ribosomal RNA, partial sequence	553	553	100%	3.00E-157	93.26%	NR_151894.1

Supplementary Materials

22	Bacteroides xylanolyticus strain X5-1 16S ribosomal RNA, partial sequence	630	630	100%	1.00E-180	96.11%	NR_104899.1
	[Clostridium] xylanolyticum strain DSM 6555 16S ribosomal RNA, partial sequence	630	630	100%	1.00E-180	96.11%	NR_037068.1
30	Alistipes senegalensis JC50 16S ribosomal RNA, partial sequence	616	616	99%	4.00E-176	95.57%	NR_118219.1
57	Flavonifractor plautii strain Prevot S1 16S ribosomal RNA, partial sequence	702	702	100%	0	99.48%	NR_043142.1
154	[Clostridium] clostridioforme strain ATCC 25537 16S ribosomal RNA, partial sequence	610	610	100%	2.00E-174	95.08%	NR_044715.2
89	Oscillibacter valericigenes strain Sjm18-20 16S ribosomal RNA, complete sequence	619	619	100%	3.00E-177	95.60%	NR_074793.2
493	Ethanoligenens harbinense YUAN-3 16S ribosomal RNA, partial sequence	544	544	100%	2.00E-154	92.01%	NR_074333.1
575	Paludicola psychrotolerans strain NC1253 16S ribosomal RNA, partial sequence	573	573	100%	2.00E-163	93.54%	NR_158111.1
242	Sporobacter termitidis strain SYR 16S ribosomal RNA, partial sequence	512	512	100%	5.00E-145	90.44%	NR_044972.1
390	Kineothrix alysoides strain KNHs209 16S ribosomal RNA, partial sequence	558	558	100%	7.00E-159	93.52%	NR_156081.1
455	[Clostridium] saccharolyticum strain WM1 16S ribosomal RNA, partial sequence	632	632	100%	0	96.37%	NR_102852.1
187	Kineothrix alysoides strain KNHs209 16S ribosomal RNA, partial sequence	675	675	100%	0	98.19%	NR_156081.1
263	[Clostridium] methylpentosum strain R2 16S ribosomal RNA, partial sequence	569	569	100%	3.00E-162	93.32%	NR_029355.1
232	Kineothrix alysoides strain KNHs209 16S ribosomal RNA, partial sequence	669	669	100%	0	97.93%	NR_156081.1
406	Lactobacillus animalis strain KCTC 3501 16S ribosomal RNA, partial sequence	684	684	99%	0	98.70%	NR_041610.1
	Lactobacillus murinus strain NBRC 14221 16S ribosomal RNA, partial sequence	684	684	99%	0	98.70%	NR_112689.1
312	Flintibacter butyricus strain BLS21 16S ribosomal RNA, partial sequence	691	691	100%	0	98.96%	NR_144611.1
11	Lactobacillus animalis strain KCTC 3501 16S ribosomal RNA, partial sequence	713	713	100%	0	100.00%	NR_041610.1
	Lactobacillus murinus strain NBRC 14221 16S ribosomal RNA, partial sequence	713	713	100%	0	100.00%	NR_112689.1
	Lactobacillus apodemi strain ASB1 16S ribosomal RNA, partial sequence	713	713	100%	0	100.00%	NR_042367.1
345	Lactobacillus faecis strain AFL13-2 16S ribosomal RNA, partial sequence	505	505	74%	9.00E-143	98.26%	NR_114391.1
94	Oscillibacter valericigenes strain Sjm18-20 16S ribosomal RNA, complete sequence	608	608	100%	6.00E-174	95.08%	NR_074793.2
188	Intestinimonas butyriciproducens strain SRB-521-5-I 16S ribosomal RNA, partial sequence	553	553	100%	3.00E-157	92.49%	NR_118554.1
516	[Eubacterium] siraeum strain ATCC 29066 16S ribosomal RNA, partial sequence	571	571	100%	8.00E-163	93.01%	NR_118675.1
573	Vallitalea pronyensis strain FatNI3 16S ribosomal RNA, partial sequence	453	453	99%	3.00E-127	88.11%	NR_125677.1
567	Lactobacillus animalis strain KCTC 3501 16S ribosomal RNA, partial sequence	459	459	97%	7.00E-129	88.62%	NR_041610.1
	Lactobacillus murinus strain NBRC 14221 16S ribosomal RNA, partial sequence	459	459	97%	7.00E-129	88.62%	NR_112689.1
	Lactobacillus apodemi strain ASB1 16S ribosomal RNA, partial sequence	459	459	97%	7.00E-129	88.62%	NR_042367.1
273	[Ruminococcus] gnavus ATCC 29149 16S ribosomal RNA, partial sequence	568	568	100%	1.00E-161	93.26%	NR_036800.1

Supplementary Materials

Supplementary figure 1. Unnormalized energy intake (expressed in kcal) of rats from experiment 1. An asterisk (*) indicates a significant different between chow and WD groups for the corresponding week in experiment 1 (*: $p<0.05$). A 2-way ANOVA was performed. Data are represented as means ± SEM.

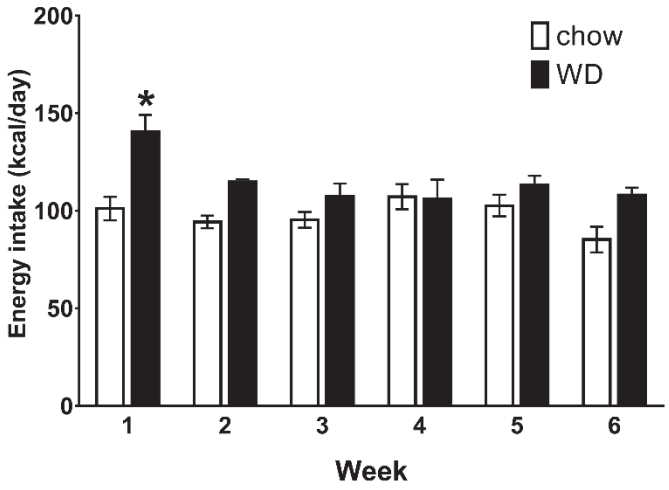

Supplementary Materials

Supplementary figure 2. Energy intake in kcal.g^{-1} of body weight (A) and in kcal (B), body weight (C) and visceral adiposity index (D) of experiment 2 conventional rats. These parameters were measured before and after WD introduction. Data are represented as means±SEM. Two different letters indicate a significant difference after 1-way ANOVA followed by Tukey's post-hoc tests.

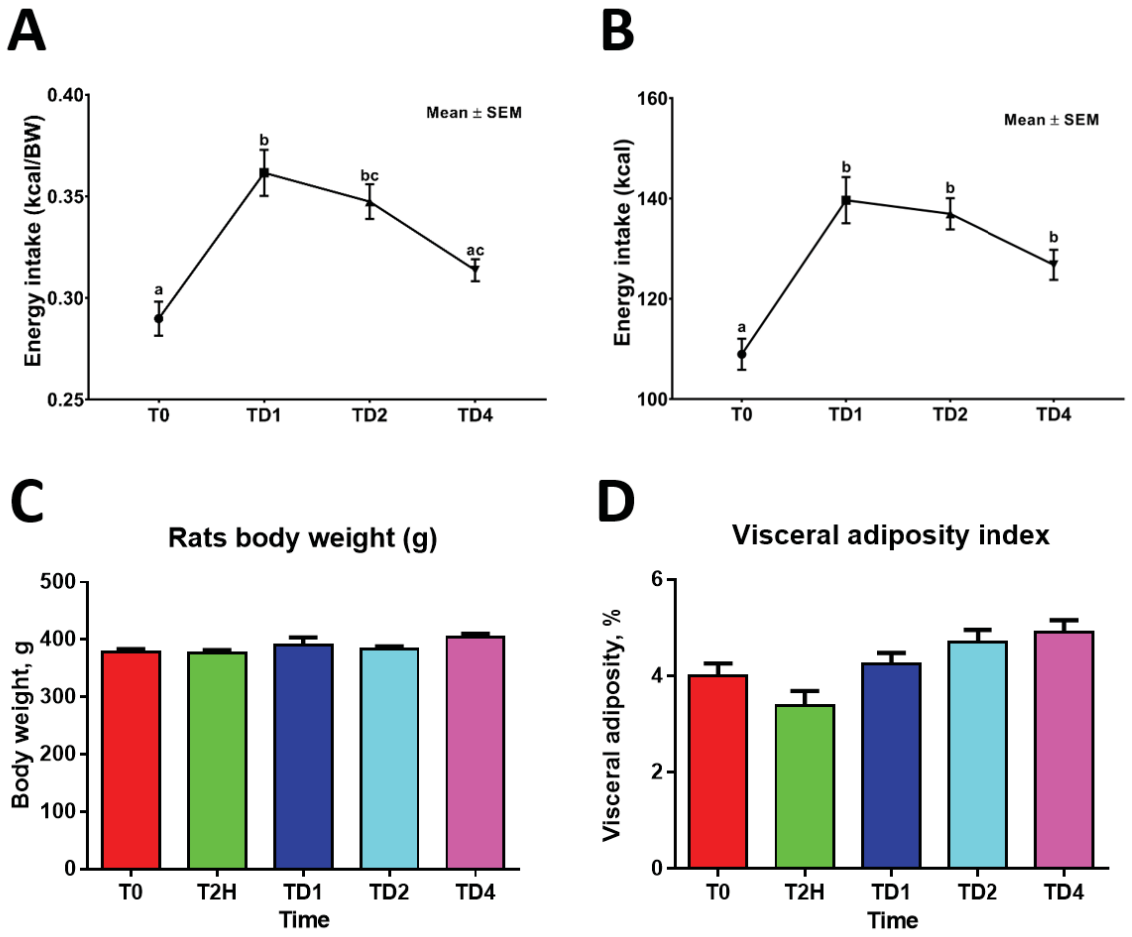

Supplementary figure 3. PLS-DA representation of hypothalamic metabolome, without T0 and T2H time groups. Represented data are normalized metabolomic data according to T0 group. Two different letters indicate a significant difference.

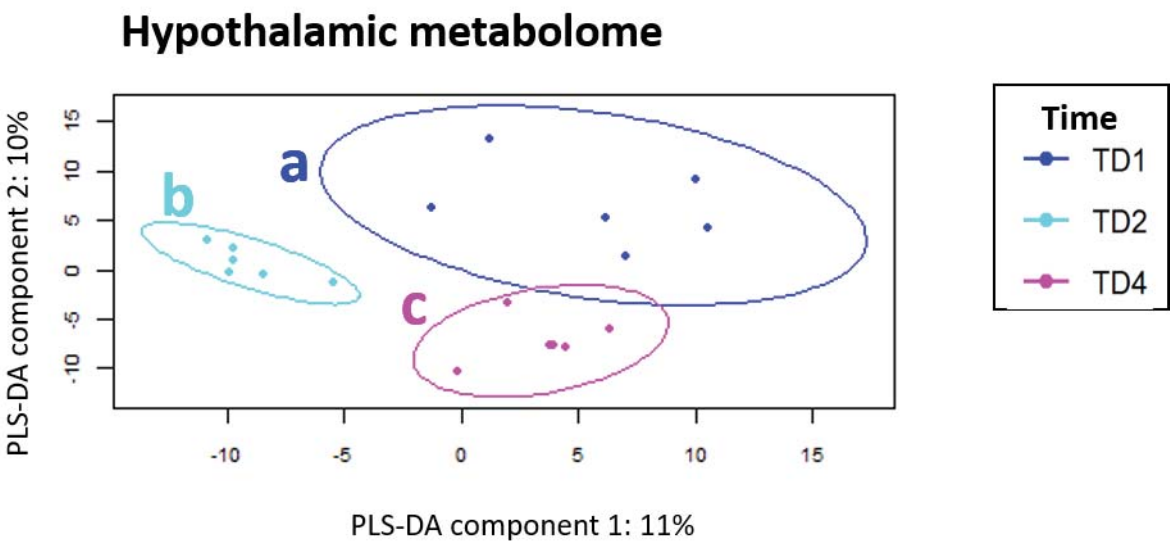

Supplementary figure 4. Relative abundances of Actinobacteria, Bacteroidetes and Firmicutes phyla across time in experiment 2. Outliers are represented as asterisks.

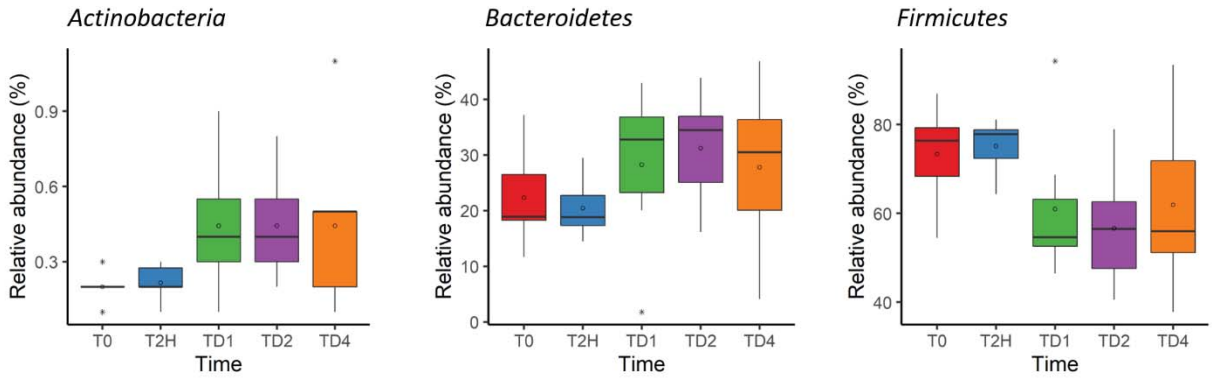

Supplementary figure 5. Energy intake in kcal of experiment 3 rats. Data are presented as means ± SEM. Dotted lines correspond to germ-free (GF) animals whereas plain lines correspond to conventional (CONV) animals, either under chow diet (grey) or WD (black). Two different letters indicate a significant statistical difference, after 2-way ANOVA followed by Tukey's post-hoc tests.

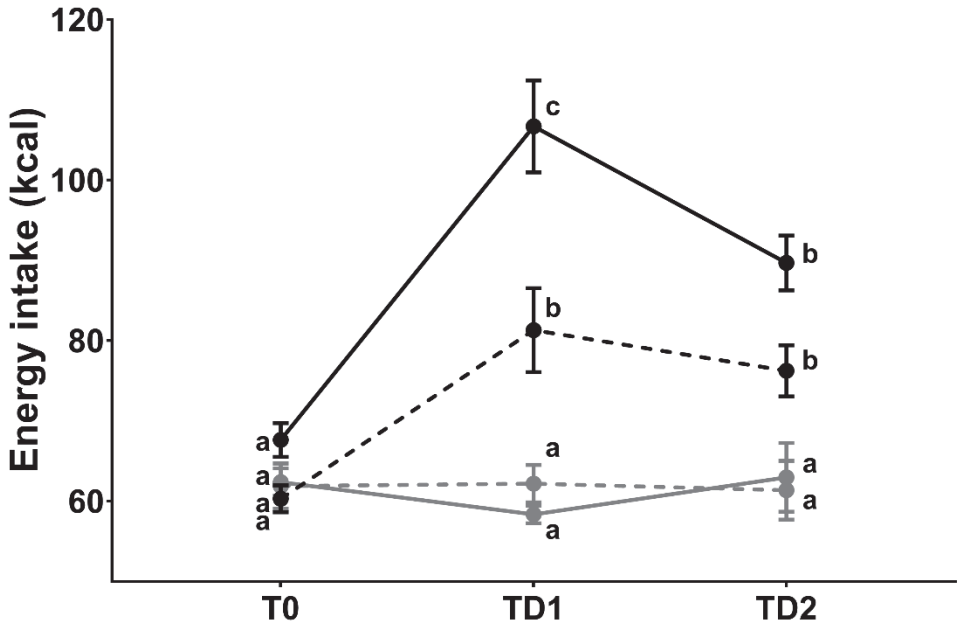

Supplementary Materials

Supplementary figure 6. Evolution of caecal microbiota after WD switch in conventional rats (experiment 3). Evolution of alpha diversity (number of observed species (A) and Shannon index (B)), β-diversity (PCoA on Bray-Curtis distance) (C), Firmicutes (D), Bacteroidetes (E), Proteobacteria (F) and *Lactobacillaceae* (G) relative abundances before and 2 days after WD introduction. N=5/group. Asterisks (*) indicate a significant difference after Mann-Whitney test performed between the two diet groups (*:P<0.05; **:P<0.01). Data beyond the end of the whiskers were considered outliers (1 point per sample). Outliers were not taken into account for statistical tests.

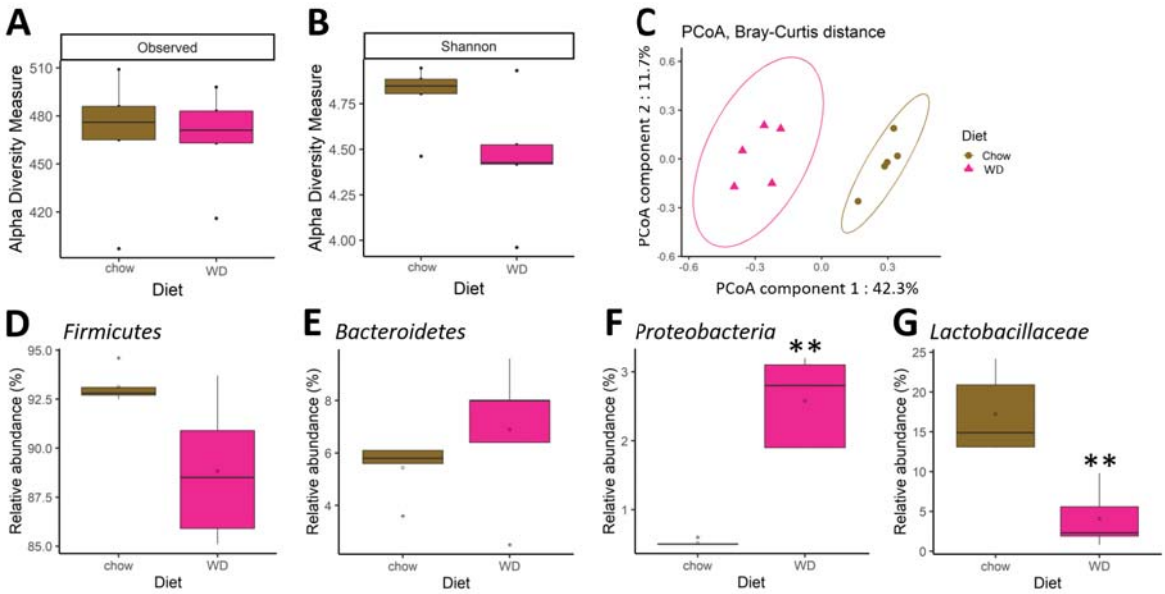

Supplementary Materials

Supplementary references

1. Callahan BJ, McMurdie PJ, Rosen MJ, Han AW, Johnson AJA, Holmes SP. DADA2: High-resolution sample inference from Illumina amplicon data. Nature Methods. 2016;13(7):581-583.

2. Chen L, Reeve J, Zhang L, Huang S, Wang X, Chen J. GMPR: A robust normalization method for zero-inflated count data with application to microbiome sequencing data. PeerJ. 2018;6:e4600.

3. McMurdie PJ, Holmes S. phyloseq: An R Package for Reproducible Interactive Analysis and Graphics of Microbiome Census Data. PLoS ONE. 2013;8(4):e61217.

4. Rohart F, Gautier B, Singh A, Lê Cao K-A. mixOmics: An R package for 'omics feature selection and multiple data integration. PLOS Computational Biology. 2017;13(11):e1005752.

5. Zoppi J., Guillaume J.-F., Neunlist M. and Chaffron S. MiBiOmics: An interactive web application for multi-omics data exploration and integration. bioRxiv. 2020.